Joint Carrier Allocation and Beamforming for Cognitive SatComs in Ka-band (17.3-18.1 GHz)

Shree Krishna Sharma*, Sina Maleki*, Symeon Chatzinotas*, Joel Grotz†, Jens Krause‡, Björn Ottersten*
*SnT - securityandtrust.lu, University of Luxembourg, Luxembourg
Email: {shree.sharma, sina.maleki, symeon.chatzinotas, bjorn.ottersten}@uni.lu
†Technical Labs, Newtec, Belgium, Email: joel.grotz@newtec.eu
‡ SES, Betzdorf, Luxembourg, Email: jens.krause@ses.com

***Abstract*—Herein, we study the spectral coexistence of Geostationary (GEO) Fixed Satellite Services (FSS) downlink and Broadcasting Satellite Services (BSS) feeder links in the Ka-band ($17.3 - 18.1$ GHz) which is primarily allocated for BSS feeder links. Firstly, a novel cognitive spectrum exploitation framework is proposed in order to utilize the available band efficiently. Subsequently, based on the interference analysis carried out between these systems, two cognitive approaches, namely Carrier Allocation (CA) and Beamforming (BF), are investigated under the considered framework assuming the availability of an accurate Radio Environment Map (REM). The employed techniques allow the flexibility of using additional shared carriers for the FSS downlink system along with the already available exclusive carriers ($19.7 - 20.2$ GHz), thus increasing the overall system throughput. It is shown that a significant improvement in the per beam throughput as well as in the beam availability can be achieved by applying CA and BF approaches in the considered scenario.**

***Index Terms*: Dual Satellite Coexistence, Cognitive SatCom, Beamforming, Carrier Assignment, Spectrum Sharing**

I. Introduction

Spectrum scarcity in Satellite Communication (SatCom) systems has become a critical issue due to the continuously increasing demand of multimedia, broadband and broadcast services, and the limited availability of the usable spectrum. Although interactive SatCom systems have moved from a single beam platform to the multi-beam, there still remains a large gap in meeting the spectral efficiency requirement of the next generation Terabit/s satellites within the 2020 horizon [1]. To address this challenge, cognitive SatComs can be an effective solution which allows the spectral coexistence of different satellite and terrestrial networks in order to improve the utilization of the available spectrum without the need of acquiring additional frequency rights [2]–[6].

The exploitation of the licensed spectrum dedicated to one system by another system in a cognitive (secondary) way can significantly enhance the utilization of the currently available spectrum [7]. However, the main problem to realize this cognitive exploitation is to provide sufficient protection to the incumbent (primary) users and to guarantee the desired Quality of Service (QoS) of the cognitive users. In this context, several contributions in the terrestrial context have studied the application of a Cognitive Radio (CR) using several approaches such as interweave, underlay and overlay [7]. These paradigms can be realized with the help of several spectral awareness mechanisms such as Spectrum Sensing (SS), Signal to Noise Ratio (SNR) estimation, database, etc. After acquiring the knowledge about spectrum availability, spectrum should be utilized effectively using suitable exploitation techniques. In this context, we study Beamforming (BF) and Carrier Allocation (CA) mechanisms to enable the coexistence of Geostationary (GEO) Fixed Satellite Service (FSS) system with Broadcasting Satellite Services (BSS) feeder links operating in the Ka band range $17.3 - 18.1$ GHz. This corresponds to one of the scenarios chosen based on market, business and technical feasibility analysis under the framework of ongoing European project FP7 project CoRaSat (Cognitive Radio for SatComs) [3].

Although there exist several contributions in the areas of CA and BF (see [8], [9] and references therein), the study of these techniques in practical scenarios is quite limited. In this context, our main contribution is to investigate and evaluate the performance of these techniques in a practical scenario considering realistic system parameters. Firstly, we propose an innovative spectrum exploitation framework in order to utilize the shared band effectively in the considered scenario. Subsequently, we present the application of our approach considering practical constraints. Finally, we evaluate the performance of the proposed framework in terms of per beam throughput and beam availability.

The remainder of this paper is structured as follows. Section II describes the considered scenario and highlights the underlying problems to be addressed. Section III proposes a novel cognitive spectrum exploitation framework. Section IV presents the interference analysis between two systems under the considered scenario while Section V proposes two exploitation mechanisms, namely BF and CA. Section VI evaluates the performance of the proposed mechanisms with the help of numerical results. Finally, Section VII concludes the paper.

II. Scenario and Problem Description

As mentioned in Section I, we consider the spectral coexistence of FSS downlink with BSS feeder links in $17.3 - 18.1$ GHz as depicted in Fig. 1. In this scenario, the BSS feeder link and FSS downlink are incumbent and cognitive links, respectively. The interference between BSS satellite and the cognitive FSS satellite can be considered to be negligible due to the provision of having fixed orbital spacing between two GEO satellites. The main interfering link in this scenario is the link from BSS feeder station to the cognitive FSS terminal, and this interference needs to be monitored effectively in order to guarantee the desired QoS of the cognitive link. Although interference may also come from the incumbent Fixed Service (FS) point to point links in the range 17.7 – 18.1 GHz, this problem has been considered in a separate study [6] and is not the focus of this paper. Therefore, the main problem in this scenario is to explore reliable CR approaches which can mitigate the harmful interference coming from the BSS feeder stations. Although there occurs no inline interference in most cases due to the underlying network topology, a significant aggregate interference may occur at a specific FSS terminal due to the side-lobes of the tranmit/receive antenna patterns. In this context, we study BF and CA techniques based on the interference analysis between these two systems as illustrated in the following sections.

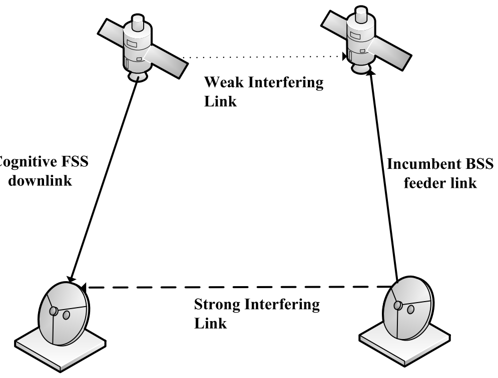

Fig. 1. Spectral coexistence of FSS downlink with BSS feeder link in the Ka-band (17.3 – 18.1 GHz)

III. Proposed Cognitive Spectrum Exploitation Framework

Among various spectrum exploitation approaches available in the literature, we follow the underlay approach in this work. Both CA and BF approaches considered in this work can be considered as underlay since they allow the simultaneous operation of the incumbent and cognitive systems in the same spectrum band, and the CR terminals do not need to find the spectral holes as in interweave systems.

Figure 2 depicts the proposed cognitive exploitation framework. Under this framework, first, interference analysis between BSS and FSS systems is carried out as described later in Section IV. Subsequently, based on the calculated interference level and the signal level obtained from the FSS system analysis, the Signal to Interference plus Noise Ratio (SINR) is computed for all the FSS terminals considering all the carrier frequencies. In this paper, we assume a database-assisted approach for our spectrum exploitation framework. In practice, the database can be available from regulators/operators or from the REMs created with the help of sensing.

Let N_{ce} be the number of carrier frequencies available in the exclusive band (19.7 – 20.2 GHz), N_{cs} is the number of carrier frequencies available in the shared band, and N_{fss} is the number of FSS terminals located within the considered coverage area. Then the total SINR matrix which describes all possible user-carrier allocations in both the shared and exclusive bands becomes of the size $N_{ct} \times N_{fss}$, where $N_{ct} = N_{ce} + N_{cs}$.

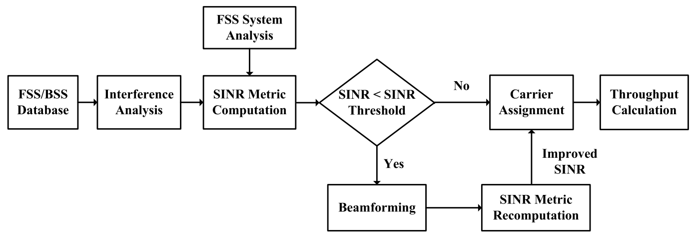

Fig. 2. Cognitive exploitation framework in the considered scenario

To implement the BF approach, an SINR threshold is defined as described later in Section V-A. We apply beamforming only in the FSS terminals whose SINR level is less than the specified threshold due to excessive interference. After applying BF, the improved SINR is fed to the CA module in order to allocate the available shared and exclusive carriers by maximizing the overall throughput as described in Section V-B.

IV. Interference Analysis

For interference analysis in the considered scenario, we consider an FSS multibeam satellite system providing coverage over a specific geographical region and focus on a representative beam of 150 km radius[1] as depicted in Fig. 3. The considered beam is centered at Betzdorf, Luxembourg (49.6833° N, 6.35° E). All the BSS feeder stations located in the Betzdorf are considered for this analysis. From the BSS database obtained from the satellite operator SES, there are altogether 21 BSS feeder links (carriers) towards 5 BSS satellites located in the GEO orbit. The locations of the FSS terminals are considered to be random and uniformly distributed over the considered representative beam. In Fig. 3, the black lines correspond to the azimuthal pointing directions of the FSS terminals with respect to the GEO FSS satellite located at 25° E and the red lines correspond to the pointing directions of the BSS feeder stations located towards five different satellites.

The received signal level at an FSS terminal is determined by carrying out the link analysis of the FSS system i.e., the link between the FSS satellite and the FSS terminals. Let P_{tfss} denotes the transmit power of the FSS satellite, then the received signal at the mth FSS terminal is given by

$$P_{r,m} = P_{\text{tfss}} G_{\text{ter}}(0) FL_{\text{fss}}(m) B(m,k), \tag{1}$$

where $G_{\text{ter}}(0)$ denotes the FSS terminal antenna gain in the boresight direction, $FL_{\text{fss}}(m) = \left(\frac{c}{4\pi D(m) f_c}\right)^2$ is the free space path loss for the satellite link with c being the speed of light, and $D(m)$ being the distance between the mth FSS terminal and the satellite, and f_c being the carrier frequency used by the FSS system. Further, $B(m,k)$ denotes the beam gain of the kth beam for the mth terminal and is given by [10], [11]

$$B(m,k) = G_{\max} \left(\frac{J_1(u(m,k))}{2u(m,k)} + 36 \frac{J_3(u(m,k))}{u(m,k)^3} \right)^2, \tag{2}$$

[1]This is merely an illustrative beam for producing performance results, and it does not necessarily have to resemble a realistic beam.

where $u(m,k) = 2.01723 \sin(\theta(m,k))/\theta_{3\text{dB}}$, J_i is the first kind of Bessel's function of order i, $G_{\max}$ is the maximum FSS satellite antenna gain, $\theta_{3\text{dB}}$ is the 3 dB angle and $\theta(m,k)$ represents the angular position of the mth user from the kth beam center with respect to the GEO satellite.

Let P_{tbss} be the transmit power of the BSS feeder station, and G_{tbss} is the gain of the BSS transmitting antenna, then the interference level received at the mth FSS terminal is given by

$$I_{\text{bss}}(m) = P_{\text{tbss}} G_{\text{tbss}}(\theta_{\text{off1}}) G_T(\theta_{\text{off2}}) FL_{\text{bss-fss}}(m), \quad (3)$$

where θ_{off1} is the offset angle (from the boresight direction) of the BSS interfering link towards the FSS terminal, θ_{off2} is the offset angle of the FSS terminal in the direction of the interfering BSS link, and $FL_{\text{bss-fss}}(m) = \left(\frac{c}{4\pi d(m) f_c}\right)^2$ with $d(m)$ being the distance between a BSS feeder station and the mth FSS terminal.

Subsequently, from (1) and (3), the SINR at the mth FSS terminal can be written as

$$SINR = \frac{P_{\text{tfss}} G_{\text{ter}}(0) B(m,k) (\frac{c}{4\pi D(m) f_c})^2}{P_{\text{tbss}} G_{\text{tbss}}(\theta_{\text{off1}}) G_{\text{ter}}(\theta_{\text{off2}}) \left(\frac{c}{4\pi d(m) f_c}\right)^2 + I_{\text{co}} + N_0}, \quad (4)$$

where I_{co} is the cochannel interference caused due to co-channel beams, $N_0 = kTB$ is the noise power calculated over bandwidth B with k being the Boltzmann's constant and T being the receiver noise temperature. In the considered scenario, bandwidths of both victim FSS and interfering BSS carriers are assumed to be 36 MHz[2]. Further, there may be more than one BSS carriers causing interference to a certain FSS carrier. For this purpose, aggregate interference needs to be calculated at the FSS terminal for a specific FSS carrier. In order to calculate the interference from the BSS carriers, interfering BSS carriers for a specific FSS carrier can be found by checking whether a BSS carrier falls within 36 MHz of the considered FSS carrier or not. If the BSS carrier falls within this range, then it is treated as an interfering carrier and is taken into account for aggregate interference calculation for the considered FSS carrier.

V. Proposed Cognitive Methods

In the following subsections, we describe our approach for the application of BF and CA methods in the considered scenario.

A. Beamforming

Several beamforming techniques have been studied in the literature in cognitive settings for different objectives such as sum rate maximization, SINR/rate balancing, and power minimization with QoS constraints etc [12]–[15]. In this paper, we focus on the Minimization of Output Energy (MOE) based approaches such as Minimum Variance Distortionless Response (MVDR) beamformer, and Linearly Constrained Minimum Variance (LCMV) beamformer. In the considered scenario, a receive beamformer can be designed at the FSS terminal in order to mitigate interference coming from BSS feeder stations. In this work, we obtain the location information of the desired and interfering terminals from the database, and thus employ a Direction of Arrival (DoA) based adaptive beamformer.

[2]The proposed framework can be straightforwardly extended to the case where FSS and BSS carrier bandwidths are asymmetric.

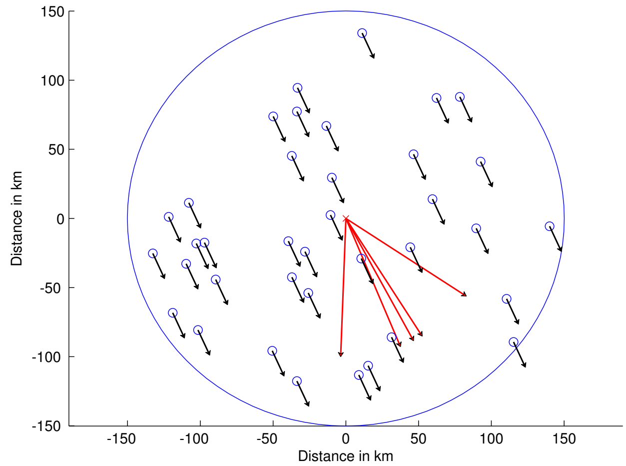

Fig. 3. Representative beam used for analyzing the FSS-BSS coexistence (The cross point (with red color) denotes the position of BSS feeder stations and small circles (with blue colour) denote the positions of FSS terminals)

The design of antenna arrays to achieve a desired performance criteria involves tradeoffs among the array geometry, the number of sensors, SNR, and Signal to Interference Ratio (SIR), as well as a number of other factors [16]. The two aspects of array design that determine its performance as a spatial filter are: (i) Array geometry, and (ii) Weight design. The first aspect establishes basic constraints upon its operation and a designer may have limited freedom to specify it due to the physical constraints involved. Regarding the second aspect, the selection of beamforming weights determines the spatial filtering characteristics of the array for the provided array geometry.

1. Antenna Structure: A terminal reflector based feed array system with 75 cm reflector diameter is considered. The antenna f/D (focal length/aperture diameter) factor is considered to be 0.6, which is typical for a consumer reflector antenna. Further, feed requirements are defined based on the sidelobe requirements to be respected. The beamforming is based on a feedback mechanism using reception quality indicators in a feedback loop to the beamforming mechanism. The assumed geometry is a typical Multiple Input LNB (MLNB) setup with 3 feeds that are aligned along the feed array horizontal line. Out of these 3 LNBs, two side feeds are offset at 2 degrees (1.91 cm) from the centered beam and are symmetrical. The reflector and feeds are aligned to provide sufficient diversity in amplitude and phase for a subsequent beamforming to work.

The important input parameter required for the beamforming design is the array response vector which depends on the angle of arrivals of interfering and desired sources. In most of the literature, this is calculated based on the assumption of Uniform Linear Array (ULA) antenna due to the availability of well-established simpler analytical expression [17]. However, in practice, the antenna structure might be different and hence the response pattern also becomes different. In the considered MLNB-based Feed Array Reflector (FAR), the response pattern of the parabolic reflector with 3 feeds is calculated using the software GRASP [18], which is widely used for the precise modelling of the reflector antennas. The feed assumptions used in the current analysis are: (i) Gaussian radiation patterns, (ii) 10 dB tapering in all directions with a taper angle of 39.5 degrees i.e., 10 dB less power at the antenna edge compared to the centre.

2. Beamforming Weight Design: The beamforming weights in the considered techniques are the functions of the covariance matrices which are functions of the array response vectors for Line of Sight (LoS) channels. In the current analysis, the amplitude and phase characteristics of the FSS terminal's front-end for a range of offset angles are obtained with the help of the GRASP tool and are subsequently used for the calculation of complex response vector of the MLNB configuration-based FAR. This complex response vector is further used for calculating beamforming weights. For the calculation of beamforming weights, the MOE based approach is followed. A similar approach has been applied in [13], [15] to design receive/transmit beamformers in terrestrial cellular-FSS multi-beam satellite coexistence in the C-band. In the following, we briefly describe the optimization problem and solutions of MVDR and LCMV beamformers under this category.

a. MVDR beamformer: The received signal at the array fed reflector can be written as

$$\mathbf{y} = \mathbf{A}\mathbf{s} + \mathbf{z}, \tag{5}$$

where $\mathbf{A} = [\mathbf{a}(\theta_1), \mathbf{a}(\theta_2), \dots, \mathbf{a}(\theta_K)]$ is an array response matrix ($\mathbf{a}(\theta)$ is the array response vector and can be obtained as described earlier in Section V-A), $\mathbf{s} = [s_1, s_2, \dots, s_K]^T$, each s_k being the symbol associated with the kth user, $\mathbf{z}$ is the Additive White Gaussian Noise (AWGN). The beamformer's response to the desired user located at an angle θ_d is given by; $\mathbf{w}^H\mathbf{a}(\theta_d)$. The optimization problem for the MVDR beamformer can be written as

$$\min_{\mathbf{w}} \mathbf{w}^H \mathbf{R}_{i+n} \mathbf{w} \quad \text{subject to} \;\; \mathbf{w}^H \mathbf{a}(\theta_d) = 1, \tag{6}$$

where $\mathbf{R}_{i+n}$ denotes the covariance matrix of interference plus noise signals. In practical scenarios, $\mathbf{R}_{i+n}$ is unavailable and only the sample covariance matrix of the received signal i.e., $\mathbf{R}_y$ is available, given by; $\mathbf{R}_y = \frac{1}{N}\sum_{i=1}^{N} \mathbf{y}(n)\mathbf{y}^H(n)$. The solution of the constrained optimization problem (6) after replacing $\mathbf{R}_{i+n}$ with $\mathbf{R}_y$ can be obtained by using Lagrange multipliers and is given by [16]

$$\mathbf{w} = \frac{\mathbf{R}_y^{-1}\mathbf{a}(\theta_d)}{\mathbf{a}^H(\theta_d)\mathbf{R}_y^{-1}\mathbf{a}(\theta_d)}. \tag{7}$$

b. LCMV beamformer: Unlike the MVDR beamformer, this includes multiple response constraints with a unity response in the desired direction and null responses in the interfering directions. The LCMV beamforming problem can be written as

$$\min_{\mathbf{w}} \mathbf{w}^H \mathbf{R}_y \mathbf{w} \quad \text{subject to} \;\; \mathbf{C}^H \mathbf{w} = \mathbf{g}, \tag{8}$$

where $\mathbf{C}$ is an $L \times K$ constraint matrix and $\mathbf{g}$ is an $L \times 1$ response vector with L being the number of feeds and K being the total number of users. The solution of the above problem is given by [16]; $\mathbf{w} = \mathbf{R}_y^{-1}\mathbf{C}(\mathbf{C}^H\mathbf{R}_y^{-1}\mathbf{C})^{-1}\mathbf{g}$.

Implementing beamforming in all the FSS terminals may cause significant overhead in terms of the system complexity. Therefore, we consider the implementation of the beamforming only in the terminals which receive harmful interference from the BSS stations. This can be done by defining an SINR threshold on the basis of modcod adaptation of the terminal under clear sky conditions. In this paper, the threshold is set in such a way that the modocod used by the FSS terminal does not degrade below 8PSK $8/15$. This corresponds to an ideal SNR value of 4.71 dB (with short XFECFRAMES at Quasi Error Free Frame Error Rate (FER) of 10^{-5}) based on the DVB-S2x specifications. In the following, we provide an algorithm to apply beamforming in the considered scenario.

Proposed algorithm for beamforming application

1) Compute the SINR matrix as described in Section IV.
2) Find the entries in the SINR matrix which are below the predefined threshold value.
3) Map the corresponding terminal positions and frequencies based on the entries from step (2).
4) For each user terminal and the corresponding frequency identified in step (3), apply MOE beamforming approach and find the corresponding SINR values for these entries.
5) Replace original entries in step (2) with the calculated ones in step (4).
6) Calculate the total throughput per beam considering the serial implementation of CA and BF module i.e., CA (See Section V-B) after BF.

B. Carrier Assignment

Let $a_{i,j} \in \{0, 1\}$ denote the $\{i, j\}$-th element of an $M \times N$ carrier assignment matrix $\mathbf{A}$ with 1 denoting the assignment of ith carrier to the jth user, with M and N elements indicating the number of available carriers and the number of FSS users, respectively. This way, $\mathbf{A}$ can be written as

$$\mathbf{A} = \begin{bmatrix} a_{11} & \dots & a_{1N} \\ \vdots & \ddots & \vdots \\ a_{M1} & \dots & a_{MN} \end{bmatrix}. \tag{9}$$

We assume that only one carrier is assigned to a single FSS user at one time instant. Therefore, we have $\sum_{i=1}^{M} a_{ij} = 1$. Similarly, the $M \times N$ SINR matrix can be written as

$$\mathbf{SINR} = \begin{bmatrix} \mathrm{SINR}_{11} & \dots & \mathrm{SINR}_{1N} \\ \vdots & \ddots & \vdots \\ \mathrm{SINR}_{M1} & \dots & \mathrm{SINR}_{MN} \end{bmatrix}. \tag{10}$$

Further, we denote by $\mathbf{R}(\mathbf{SINR})$ the rate matrix with $r_{ij},\ i = 1, \cdots, M,\ j = 1, \cdots, N$ elements indicating the associated DVB-S2X rate [19]. Now the CA problem is to find the value of a_{ij} in $\mathbf{A}$ which maximizes the overall throughput of the system. This problem can be expressed in the following form

$$\max_{\mathbf{A}} || \operatorname{vec}(\mathbf{A} \odot \mathbf{R}(\mathbf{SINR}))||_1 \quad \text{subject to} \;\; ||\mathbf{A}_j||_1 = 1, \tag{11}$$

where $\odot$ denotes the Hadamard product, $\operatorname{vec}(\cdot)$ denotes the vectorization operation, $\mathbf{A}_j$ denotes the jth column of $\mathbf{A}$,

TABLE I. SIMULATION AND LINK BUDGET PARAMETERS

Parameter	Value
Carrier bandwidth	36 MHz
Shared band	17.3 GHz to 18.1 GHz
Exclusive band	19.7-20.2 GHz
Parameters for FSS system	
Satellite orbital position	$25^{\circ} E$
Satellite EIRP	61 dBW
Terminal Gain	42.1 dBi
Antenna pattern of FSS terminal	ITU-R S.465
FSS receiver noise temp.	262 K
Noise power	-128.8552 dBW@36MHz
Co-channel margin	-13 dBW
Reuse pattern	4 color (freq./pol.)
Channel	LoS channel (path loss+beamgain matrix)
Satellite height	35786 km
Parameters for BSS Feeder Station	
Transmit power	19 dBW
Antenna gain	62 dBi@17.7 GHz
Antenna pattern	ITU RR Appendix 7
Location	$49.6833^{\circ} N, 6.35^{\circ} E$
Number of BSS carriers	21

and $||\cdot||_1$ denotes the norm 1 operator. To solve the above optimization problem, we employ the widely used Hungarian algorithm in order to assign each user to a carrier in such a way that the overall throughput of the considered system is maximized [20].

VI. PERFORMANCE EVALUATION

1. Simulation Environment: In this section, we evaluate the performance of BF and CA approaches in the considered co-existence scenario. The considered system set-up is described in Section IV (See Fig. 3). Further, we present link budget and simulation parameters for FSS and BSS systems in Table I. In the considered system set up, the shared band ($17.3 - 18.1$ GHz) is divided into 23 subbands in the interval of 36 MHz and the FSS exclusive band is divided into 14 subbands in the interval of 36 MHz. Subsequently, 37 randomly placed FSS terminals were considered within the circular area of radius 150 km and the corresponding SNR matrices were obtained considering all the carrier-user combinations for both shared and exclusive cases. In the shared band, SINR matrix was constructed by considering interference from the BSS carriers. Then the SINR level at each FSS terminal is calculated by following the analysis provided in Section IV.

For our numerical analysis, we consider the following cases: (i) Case 1: Exclusive only, (ii) Case 2: Shared plus exclusive without BSS interference, and (iii) Case 3: Shared plus Exclusive with BSS interference. Out of the above cases, Case 1 denotes the conventional system without the use of any shared carriers. Case 2 represents the scenario where the additional spectrum is allocated to the FSS system. This case does not exist in practice but is considered for the comparison purpose. Further, Case 3 depicts the scenario where BSS and FSS systems share the band $17.3 - 18.1$ GHz primarily allocated to the BSS system. Additionally, we divide the Case 3 into the following 3 subcases: (a) Subcase 31: without CA, (b) Subcase 32: with CA, and (c) Subcase 33: with CA plus BF.

2. Numerical Results: We present the per beam throughput comparison of the above cases and subcases in Table II. From the table, it can be observed that the exploitation of the shared band with the considered approach provides significant gain in terms of the per beam throughput. More specifically, the

TABLE II. PER BEAM THROUGHPUT COMPARISON OF VARIOUS APPROACHES

Cases	Value (Gbps)
Exclusive only w/ CA (**Case 1**)	0.761
Shared plus Exclusive w/o BSS int. w/ CA (**Case 2**)	2.0006
Shared plus Exclusive w/ BSS int. w/o CA (**Subcase 31**)	1.8357
Shared plus Exclusive w/ BSS int. w/ CA (**Subcase 32**)	1.9916
Shared plus Exclusive w/ BSS int. w/ CA+BF (**Subcase 33**)	2.1388
Comparison of cases	**Improvement (%)**
Improvement of **Subcase 32** over **Subcase 31**	8.49 %
Improvement of **Subcase 32** over **Case 1**	161.70 %
Improvement of **Subcase 33** over **Case 1**	181.05 %
Improvement due to **BF** w. r. t. **Case 1**	19.35 %

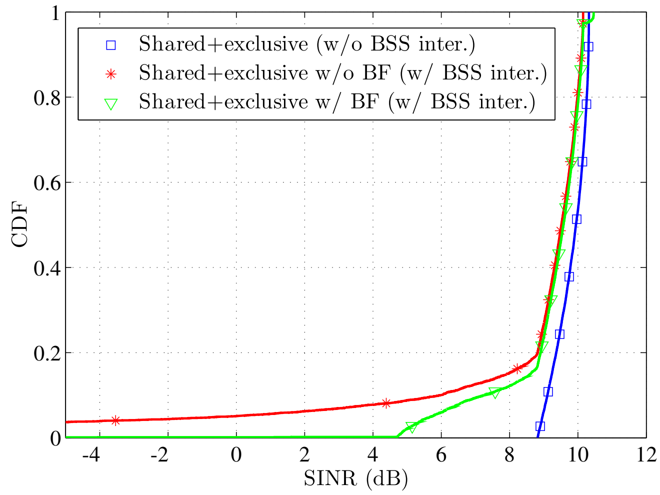

Fig. 4. CDF plots of SINR distribution with and without beamforming

main observations from Table II are highlighted below. The application of CA method in the shared plus exclusive bands provides 8.49 % improvement over the case without the CA in the presence of BSS interference. Further, the flexibility of using the shared bands using the CA approach provides around 161.70 % improvement over the exclusive only case. Moreover, if we apply BF before performing the CA, we get additional gain of 19.35 % with respect to the exclusive only throughput, which is a considerable gain. It should be highlighted here again that not all FSS terminals have to employ beamforming approach. Only a few terminals which receive low SINRs ($<$ 4.71 dB) implement the beamforming technique. In addition, it should be noted that the gain achieved by beamforming further increases in the scenarios where interference is denser i.e., multiple BSS sites on the same beam.

In addition to the throughput improvement, the proposed CA and BF approaches also significantly enhance the beam availability as illustrated in Figs. 4 and 5 as described below. Figure 4 depicts the Cumulative Distribution Function (CDF) plots of SINR distribution with and without beamforming considering the presence and the absence of BSS interference. The SINR values plotted in this figure were obtained with random carrier assignment considering the worst case scenario i.e., without applying the proposed CA approach. More specifically, the SINR vector for each case was obtained by taking the minimum over all the carrier frequencies in the calculated SINR matrix. It can be noted that the SINR distribution degrades in the presence of the BSS interference. More specifically, in the presence of BSS interference, almost

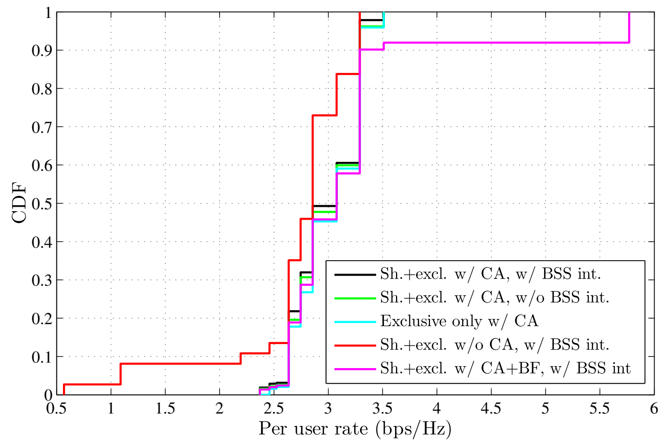

Fig. 5. CDF of the per user rate in bps/Hz for different cases

10 % users have SINR less than 6 dB and about 5 % users have SINR less than 0 dB in the considered FSS-BSS coexistence scenario. From the figure, it can be observed that by applying the beamforming approach at the selected terminals, the beam availability can be considerably improved.

Furthermore, Fig. 5 provides the CDF plots of the per user rate for the considered cases in bps/Hz. The user rates plotted in this figure were calculated by applying the CA method described in Section V-B. From the figure, it can be depicted that by employing the CA, the beam availability in the presence of the BSS interference approaches the availability that would be obtained in the absence of the BSS interference. More specifically, the minimum rate increases from the value of 0.567 bps/Hz to the value of 2.37 bps/Hz while employing the CA scheme, which is a significant improvement in the user fairness (expressed in terms of the minimum user rate). Further, the BF approach provides more than 3.5 bps/Hz to almost 8 % users i.e., it allows these users to use higher modcod than in the other cases as depicted in Fig. 5.

VII. Conclusions and Future Work

In this paper, the coexistence of BSS feeder links and FSS satellite downlink has been studied using a novel spectrum exploitation framework. Based on the SINR levels of the FSS terminals, CR approaches such as beamforming and CA have been applied in order to tackle the problem of the BSS interference. It has been noted that per beam throughput as well as the beam availability can be significantly improved by employing the proposed approaches. More specifically, the BF approach provides an additional gain of 19.35 % over the gain of 161.70 % that would be achieved with the CA only approach with respect to the exclusive only case. In order to avoid BF complexity, one can implement only CA approach in the considered scenario while still achieving a significant per beam throughput gain over the conventional exclusive only system. In our future works, we plan to perform the system level analysis of the FSS system considering the proposed framework and to apply the considered approaches in the dense interference scenarios e.g., FSS-Fixed Service (FS) terrestrial link coexistence scenario.

Acknowledgement

This work was partially supported by the EU FP7 project CoRaSat and by National Research Fund, Luxembourg under CORE project SeMIGod.

References

[1] O. Vidal and et al, "Next generation high throughput satellite system," in *IEEE First AESS European Conference on Satellite Telecommunications (ESTEL)*, Oct. 2012, pp. 1–7.

[2] S. K. Sharma, S. Chatzinotas, and B. Ottersten, "Satellite cognitive communications: Interference modeling and techniques selection," in *6th ASMS and 12th SPSC*, Sept. 2012, pp. 111–118.

[3] K. Liolis and et al, "Cognitive radio scenarios for satellite communications: The corasat approach," in *Future Network and Mobile Summit (FutureNetworkSummit), 2013*, July 2013, pp. 1–10.

[4] S. K. Sharma, S. Chatzinotas, and B. Ottersten, "Cognitive radio techniques for satellite communication systems," in *IEEE 78th Vehicular Technology Conference (VTC Fall)*, Sept. 2013, pp. 1–5.

[5] M. Hoyhtya and et al, "Applicability of cognitive radio to satellite systems (ACROSS)," VTT technical research centre, Finland, Tech. Rep., 2012. [Online]. Available: http://telecom.esa.int/telecom

[6] S. K. Sharma, S. Maleki, S. Chatzintoas, J. Grotz, and B. Ottersten, "Implementation aspects of cognitive techniques for Ka band (17.7-19.7 GHz) SatComs," in *7th ASMS/13th SPSC*, Sept. 2014.

[7] A. Goldsmith, S. Jafar, I. Maric, and S. Srinivasa, "Breaking spectrum gridlock with cognitive radios: An information theoretic perspective," *Proceedings of the IEEE*, vol. 97, no. 5, pp. 894 –914, May 2009.

[8] E. Z. Tragos, and et al, "Spectrum Assignment in Cognitive Radio Networks: A Comprehensive Survey," IEEE Communications Surveys & Tutorials, vol. 15, no. 3, pp.1108-1135, 2013.

[9] S.-M. Cai and Y. Gong, "Cognitive beamforming for multiple secondary data streams with individual snr constraints," *IEEE Trans. Signal Process.*, vol. 61, no. 17, pp. 4189–4198, Sept 2013.

[10] M. Diaz, N. Courville, C. Mosquera, G. Liva, and G. Corazza, "Non-linear interference mitigation for broadband multimedia satellite systems," in *Int. Workshop on Satellite and Space Commun.*, Sept. 2007, pp. 61 –65.

[11] S. K. Sharma, S. Chatzinotas, and B. Ottersten, "Interference alignment for spectral coexistence of heterogeneous networks," *EURASIP J. Wireless Commun. and Networking*, vol. 46, 2013.

[12] A. Tajer, N. Prasad, and X. Wang, "Beamforming and rate allocation in miso cognitive radio networks," *IEEE Trans. Signal Process.*, vol. 58, no. 1, pp. 362–377, 2010.

[13] S. K. Sharma, S. Chatzinotas, and B. Ottersten, "Transmit beamforming for spectral coexistence of satellite and terrestrial networks," in *8th Int. Conf. CROWNCOM*, July 2013, pp. 275–281.

[14] K. Cumanan, L. Musavian, S. Lambotharan, and A. Gershman, "SINR balancing technique for downlink beamforming in cognitive radio networks," *IEEE Signal Processing Letters*, vol. 17, no. 2, pp. 133–136, 2010.

[15] S. K. Sharma, S. Chatzinotas, and B. Ottersten, "Spatial filtering for underlay cognitive satcoms," in *5th Int. Conf. Personal Satellite Services*, June 2013.

[16] H. L. V. Trees, *Optimum Array Processing: Detection, Estimation and Modulation Theory*. Wiley, 2002, Part IV.

[17] H. Krim and M. Viberg, "Two decades of array signal processing research: the parametric approach," *IEEE Signal Process. Magazine*, vol. 13, no. 4, pp. 67–94, July 1996.

[18] GRASP, http://www.ticra.com/products/software/grasp, 2000.

[19] DVB, "Digital video broadcasting (DVB); second generation framing structure, channel coding and modulation systems for broadcasting, interactive services, news gathering and other broadband satellite applications, Part II: S2-Extensions (DVB-S2X) - (Optional)," March 2014.

[20] H. W. Kuhn, "The Hungarian method for the assignment problem," *Naval Research Logistics Quarterly*, vol. 2, pp. 83–97, 1955.